

Probing the Galactic Halo with Globular Cluster Tidal Tails

Carl J. Grillmair

*Jet Propulsion Laboratory, Mail Stop 183-900, 4800 Oak Grove Drive,
Pasadena CA 91109*

Abstract. We discuss recent observational and numerical work on tidal tails in globular clusters. Evidence of tidal tails has now been found in 16 Galactic globulars and 4 globulars in M31. Simulations indicate that mapping of these tidal tails over most of a typical cluster's orbit may be quite feasible. A relatively modest effort in this regard would yield reliable space velocities for those clusters whose tidal tails could be traced to angular separations of a few degrees or more. Mining of forthcoming databases should allow us to trace the individual orbital paths of globular clusters over large portions of the sky. This would enable us to better constrain models of the collapse of the Galaxy and to build up an accurate picture of the distribution of matter in the Galactic halo.

1. Introduction

Globular clusters have long been known to be limited in extent by the tidal stresses imposed by the potential field of the Galaxy. King (1966) developed a remarkably successful model for globular clusters in which the spatial extent of a cluster (the "tidal radius" = r_t) is determined by the strength of Galactic tidal forces at the cluster's perigalacticon. Extensive campaigns to measure the radial surface density profiles of globular clusters using aperture photometry and star counts (e.g. Kron & Mayall 1960; King et al. 1968; Peterson 1976, Hanes & Brodie 1985) determined that the form of the profiles appeared to be in agreement with King models over several orders of magnitude for almost all clusters observed.

The direct relationship between the tidal radius and the orbital perigalactic distance assumed by King prompted other investigators to try to measure individual globular cluster orbit shapes (or conversely the potential field of the Galaxy) using the tidal radii computed from fits of King models to the data (e.g. Peterson 1974; Innanen, Harris, & Webbink 1983). However, it was soon realized that the uncertainties in both the published profiles and in our understanding of weak tidal encounters severely hindered this type of analysis. With the advent of parallel computer architectures, more efficient N-body codes, fast plate-scanning machines, and large-format CCD detectors, great strides have been made on both these fronts. It may not be altogether surprising that many of the questions we had once asked may turn out to be largely irrelevant to the problems we ultimately want to solve.

2. Numerical Work

Globular cluster evolution and the process of tidal stripping have been addressed many times both analytically and numerically (see for example Spitzer 1987 and references therein; Lee & Ostriker 1987; Allen & Richstone 1988, McGlynn 1990; McGlynn & Borne 1991). Many works have focussed on the stability of various types of stellar orbits under the influence of tidal forces, and the consensus is that the short-term effects of tidal processes on clusters are considerably more complicated than the simple binding energy cutoff assumed in the King model. The question of whether r_t accurately predicts the eventual limiting radii of clusters is still a source of some contention, with proponents favoring values ranging from $0.5r_t$ to r_t .

More recent work on weak tidal encounters utilizing both the Fokker-Planck approach (Oh & Lin 1992; Lee & Goodman 1995) and self-consistent, large-scale N-body techniques (Grillmair et al. 1998) confirm that tidal stripping is not a very efficient process and that only a fraction of unbound or marginally-bound particles are removed in any particular tidal encounter. Combined with continual two-body relaxation in the core of the cluster and the consequent replenishment of the region near r_t , a long-term, episodic flow of particles away from the cluster should be expected. Given the very low escape velocities near r_t , stripped particles may remain in the vicinity of the cluster for several galactic orbits. Depending on which end of the equipotential surface the escaping particles passed through, they would then either migrate ahead of the cluster or fall behind, giving rise to slowly growing tidal tails. Figure 1 shows one of Grillmair et al.'s model clusters after 30 eccentric orbits in a spherical, logarithmic potential.

The effects of a disk were not considered in the works cited above, but disk shocking of the cluster is expected to variously enrich, broaden, and lengthen the tidal tails as a result of heating of the outer parts of the cluster (e.g. Murali & Weinberg 1997). In addition, irregularities in the Galactic disk such as giant molecular clouds will tend to scatter stars already in the tidal tails. Nonspherical galactic potentials would similarly tend to broaden the tidal tails as the orbits of stars precess independently of one another. Further modeling work should be aimed at studying the observable consequences of these processes, of using realistic stellar mass distributions (e.g. Johnstone 1993; Lee & Goodman 1995), and at better addressing the survival statistics of globular clusters in the face of continual weak tidal encounters.

3. Observations

Early work on defining the limits of globular clusters through star counts were limited by the \sqrt{N} uncertainties introduced by the large number of foreground and background stars. Using photographic plates taken in two colors, Grillmair et al. (1995) were able to reduce this foreground/background contamination by 90% or more by selecting stars based on their colors and magnitudes. Most of the globular clusters in their sample were found to depart from the form predicted by King models, with an excess surface density of stars at large r and significant numbers of stars with $r > r_t$. Figures 2 and 3 show the one and two-dimensional distributions of color-selected stars around NGC 7089. The departures in the

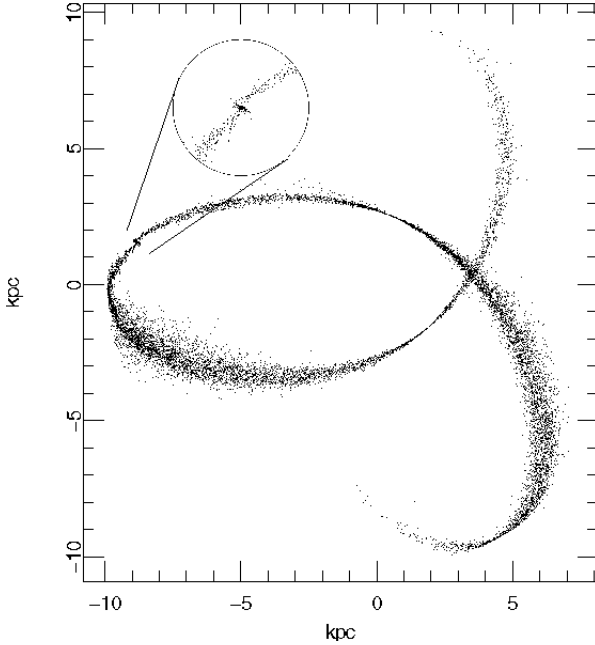


Figure 1. A 64K-particle cluster in a spherical, logarithmic potential (centered at the origin) after 30 orbits. The cluster (at left center) survives despite having lost nearly 75% of its initial mass. The inset shows the region near the cluster magnified to reveal the signature plumes of the most recent perigalactic passages.

surface density profiles are similar both qualitatively and quantitatively to the numerical results, with a “break” from a King profile at $r < r_t$ followed by a powerlaw decline which varies from cluster to cluster. This variation in the power-law component is consistent with the modeling results of Grillmair et al. (1998), who found that the gradient in the extended surface density profile depends both on the shape of the cluster’s orbit and, through conservation of energy and angular momentum, on the orbital phase of the cluster. At some level (which depends on the rate of evaporation of stars and on the orbit’s orientation with respect to our line of sight) the tidal tails will obscure the tidal cutoffs predicted by King-Michie models.

Evidence of tidal tails has now been found in 16 Galactic globular clusters, including M2, M15, NGC 288, NGC 362, NGC 1904, NGC 4590, NGC 5824, NGC 6864, NGC 6934, NGC 6981 (Grillmair et al. 1995), M5, M12, M13, M15, NGC 5466 (Lehmann & Scholz 1996), M5 (Kharchenko, Scholz, & Lehmann 1997), M55 (Zaggia, Piotto, & Capaccioli 1997), and ω Cen (Leon & Meylan 1997). Efforts are underway to extend this sample, and to trace known tidal tails beyond the 2° or less to which existing data have been limited. Interestingly, tidal tails have recently also been detected in four globular clusters in M31 (Grillmair et al. 1996; Holland, Fahlman, & Richer 1997). The decline in the number of blue foreground stars at $V > 23$, combined with both a large projected field of view and spatial resolution sufficient to distinguish between stars and galaxies, makes this a fairly straightforward endeavor using the Wide Field Planetary Camera 2 on the Hubble Space Telescope.

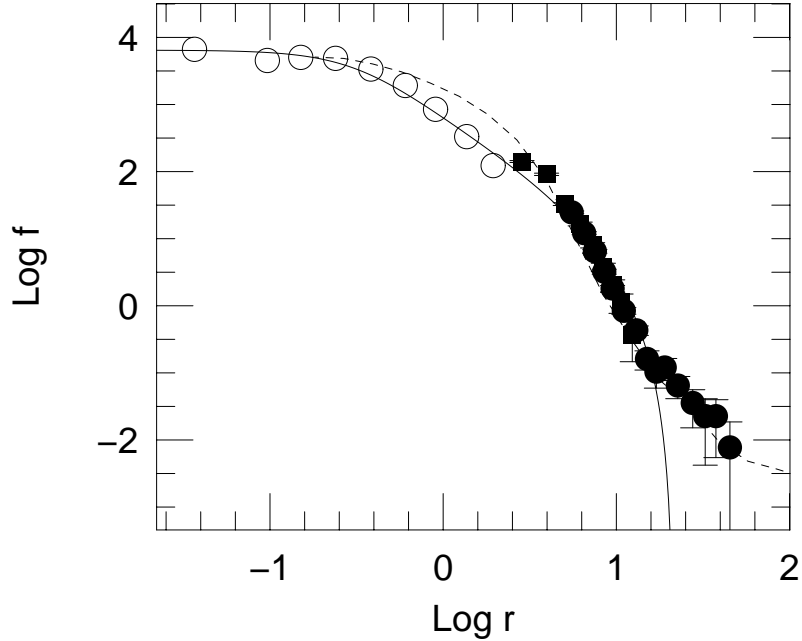


Figure 2. Surface density profile of NGC 7089 (=M2). Open circles represent aperture photometry of Hanes & Brodie (1985), filled squares and filled circles show the star counts of King et al. (1968), and of Grillmair et al. (1995). The best-fit King model is shown by the solid line, and the dashed line shows one of Grillmair et al.'s (1998) models arbitrarily normalized to the data at large r . Departures at small radii reflect the differences between King models and the Jaffe model used in the numerical experiments. Note the break near the tidal radius and the power-law decline at large r characteristic of tidal tails.

Given the faintness of the stars which make up the bulk of the tidal tails and the fact that they constitute only a small fraction of the color-selected field stars, obtaining spectra would be more than a minor undertaking. Nonetheless, spectra would be useful both to confirm association of these stars with their parent clusters and, by examining their velocity distributions, to study the interaction of the cluster and Galactic potentials. Indeed, in a sample of 237 stars in the outskirts of M15, Drukier et al. (1998) find that the velocity dispersion appears to have a minimum at about 7 arcminutes, well inside the 23 arcminute tidal radius of the cluster. These authors favor tidal heating as being responsible for a subsequent slight rise in the velocity dispersion. It is also possible that their sample includes a small number of stars residing in the unbound halo or the tidal tail and projected along our line of sight.

Interestingly, the tidal tails observed to date imply that globular clusters cannot be surrounded by halos of dark matter. Moore (1996) showed for NGC 7089 that the existence of the tidal tails requires a global mass-to-light ratio of $M/L < 2.5$, consistent with values for M/L derived for the central regions of globular clusters.

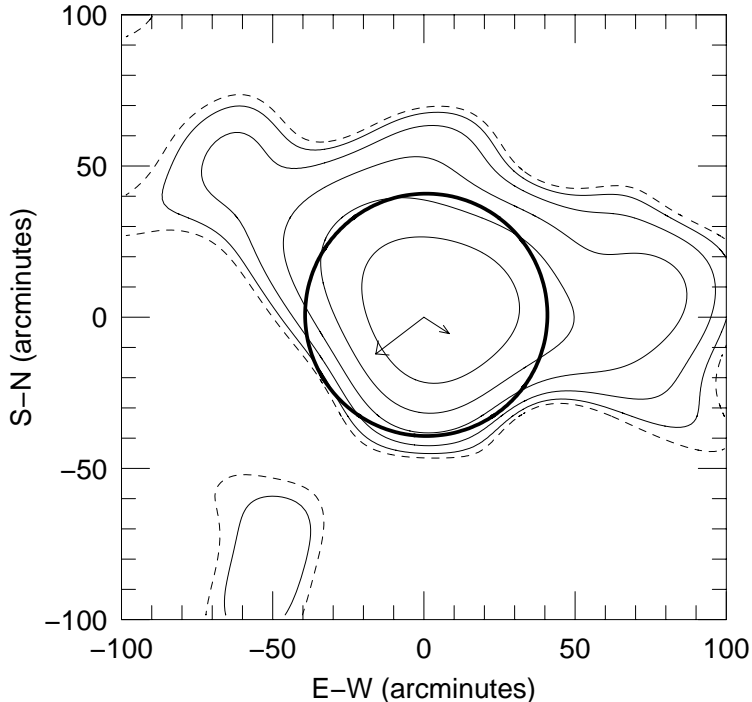


Figure 3. Contours of the color-magnitude-selected star distribution around NGC 7089 after smoothing with a Gaussian kernel with $\sigma = 20$ arcminutes. The heavy line shows the extent of the best-fit King model after the same degree of smoothing and at a surface density level equal to that shown by the dashed line.

4. Tracing Cluster Orbits

The presence of tidal tails give us a potentially useful tool for determining cluster orbits and mapping the Galactic potential field. Mining large data sets like the Guide Star Catalog II will soon make it possible to trace tidal tails to large angular distances from their parent clusters. Figure 4 shows the surface density distribution in one of Grillmair et al.’s (1998) 64K-particle models as it might appear on the sky from our Galactic vantage point. The surface density of particles has been scaled to approximately match the observed number of stars in NGC 7089. If, as is the case for this particular model, NGC 7089 has lost the majority of its original stars to its tidal tails, we would expect to find $\sim 10^6$ stars brighter than $V = 23$ strewn along this single cluster’s orbit. The highest surface densities in Figure 4 (with the exception of the cluster itself) correspond to an apogalactic portion of the cluster orbit and to projection of the tail along our line of sight. With suitably optimized color-selection criteria, and with the exception of regions very near the Galactic plane, it would be quite feasible to follow such tails for most of their length.

More challenging will be the issue of confusion. There are probably many hundreds of apogalactic, high-density swarms of blue turnoff stars laid down by old halo clusters. Determining their orientations in the presence of contamination by unaffiliated halo stars and unresolved galaxies and matching such tail segments with parent clusters may well not be trivial. Simulations show that the solution will most often be to obtain the deepest photometry possible, both to minimize photometric errors and thereby keep the color-magnitude selection

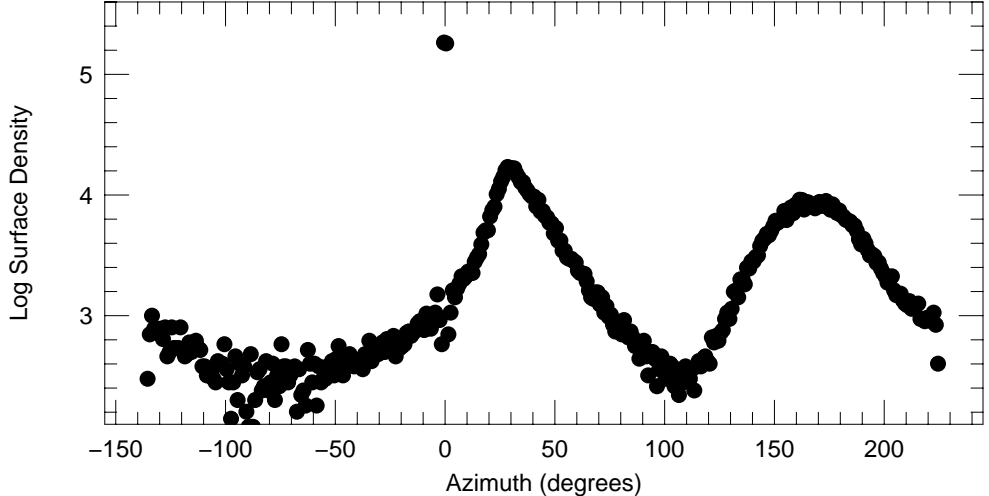


Figure 4. The number of stars per square degree down to $V = 23$ measured along the tidal tails of a simulated cluster. The cluster is viewed at some arbitrary point along an orbit inclined 45° with respect to the plane of the Galaxy, and the surface densities are scaled to match the number of *cluster* stars in NGC 7089.

criteria as restrictive as possible, and to take advantage of the fainter end of the globular cluster luminosity function.

Another reason for going deep is to reduce the uncertainties in photometrically determined distances. While the turnoff regions of most globular clusters stand out rather well from the distributions of Galactic field stars, this region is less useful for determining relative distances via main sequence fitting. Figure 5 shows a simulation based on a model of Grillmair et al. (1998) wherein particles have been assigned colors and magnitudes using a typical metal-poor globular cluster isochrone and luminosity function. Assuming reasonable exposure times on a 1-meter Schmidt-type telescope and applying appropriate uncertainties, we recover photometric distances down to a limiting apparent magnitude of $V \sim 23$ (or about 3 magnitudes below the turnoff). Despite the photometric errors and the uncertainty in absolute stellar luminosities in the region near the turnoff, Figure 5 shows that the cluster's orbit can be readily traced over most of the extent of the tidal tails. Globular cluster orbit shapes can thus be determined on a case by case basis, rather than with the statistical arguments used in the past.

Knowing a cluster's line-of-sight velocity, the orbital path of the cluster as deduced from its tidal tails immediately yields a reasonably accurate value for the cluster's space velocity; the orientation of the tidal tails on the sky near the cluster gives the second component of the velocity and the photometric distances of stars in the tails yield the third. Conservation of orbital angular momentum then allows us to compute the space velocity at any point along the tidal tails (we neglect here the small error introduced by the fact that the orbits of stars in the tidal tails do not exactly coincide with that of the cluster). The halo potential itself must be determined numerically (e.g. Binney and Tremaine 1987). Using normal points derived from Figure 5 we recover the spherical model potential to within 10% over the radial range sampled by the orbit. Since the Galactic halo potential is non-Keplerian and is quite probably nonspherical as well, even a well-determined globular cluster orbit will not be

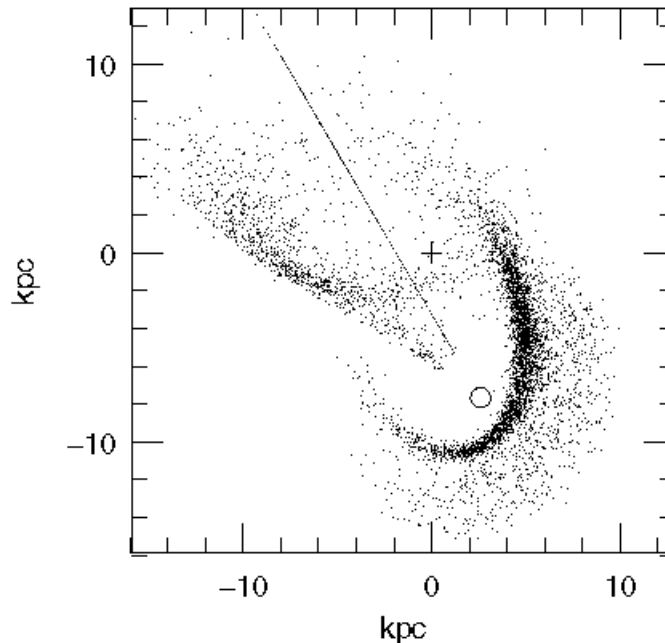


Figure 5. Simulation of a typical orbital trace using photometric distances to tidal tail stars. The open circle denotes the location (projected onto the plane of the cluster’s orbit) of our solar system, and the Galactic center resides at the origin. The cluster’s position is indicated by the “finger of God” resulting from photometric uncertainties. Note that the effects of sample contamination by field stars (which will vary hugely from one orbit to the next) are not included here.

sufficient to map the potential at this level of accuracy. However, tracing the orbits of several clusters would provide strong constraints on the distribution of matter in the inner portion of the Galactic halo. Combining these orbit shapes and mass distributions with similar information gleaned from the tidal tails of the Milky Way’s satellite galaxies (Johnston, Hernquist, & Bolte 1996) would greatly improve our understanding of the initial collapse and subsequent evolution the Galaxy.

References

- Allen, A. J., & Richstone, D. O. 1988, *ApJ*, 325, 583
- Binney, J., & Tremaine, S. 1987, *Galactic Dynamics*, Princeton University Press: Princeton.
- Drukier, G. A., Slavin, S. D., Cohn, H. N., Lugger, P. M., & Berrington, R. C. 1998, *AJ*, in press.
- Grillmair, C. J., Freeman, K. C, Irwin, M., & Quinn, P. J. 1995, *AJ*, 109, 2553
- Grillmair, C. J., Ajhar, E., Faber, S. M., Baum, W. A., Lauer, T. R., Lynds, C. R., & O’Neil, E. Jr. 1996, *AJ*, 111, 2293
- Grillmair, C. J., Quinn, Freeman, K. C., Salmon, J., Prince, T., & Messina, P. 1998, in preparation.
- Hanes, D. A., & Brodie, J. P. 1985, *MNRAS*, 214, 491
- Holland, S., Fahlman, G. G., & Richer, H. B. 1997, *AJ*, 114, 1488

- Innanen, K. A., Harris, W. E., & Webbink, R. F. 1983, AJ, 88, 338
Johnston, K. V., Hernquist, L., & Bolte, M, 1996, ApJ, 465, 278
Johnstone, D. 1993, AJ, 105, 155
Kharchenko, N., Scholz, R.-D., & Lehmann, I. 1997, A&AS, 121, 439
King, I. R. 1966, AJ, 71, 276
King, I. R., Hedemann, E., Hodge, S. M., & White, R. E. 1968, AJ, 73, 456
Kron, G. E., & Mayall, N. U. 1960, AJ, 65, 58
Lee, H. M., & Ostriker, J. P. 1987, ApJ, 322, 123
Lee, H. M., & Goodman, J. 1995, ApJ, 443, 109
Leon, S., & Meylan, G. 1997, personal communication.
McGlynn, T. A. 1990, ApJ, 281, 184
McGlynn, T. A., & Borne, K. D. 1991, ApJ, 372, 31
Moore, B. 1996, ApJ, 461, L13
Murali, C., & Weinberg, M. D. 1997, MNRAS, 291, 717
Oh, K. S., & Lin, D. N. C. 1992, ApJ, 386, 519
Peterson, C. J. 1974, ApJ, 190, L17
Peterson, C. J. 1976, AJ, 81, 617
Spitzer, L. 1987, *Dynamical Evolution of Globular Clusters*, Princeton University Press: Princeton.
Zaggia, S., Piotto, G., & Capaccioli, M. 1997, A&A, 327, 1004